

Broad overview

- Extinction vs. attenuation
 - The Calzetti Starburst attenuation law
 - The importance of dust Geometry
 - Meurer IRX-beta relation
-

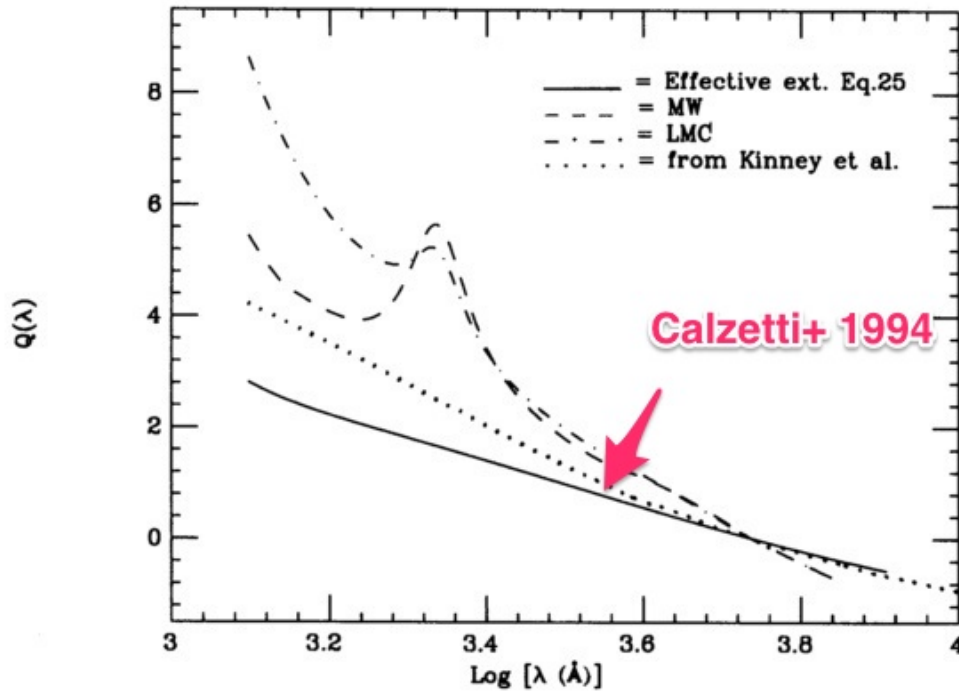


FIG. 21.—The extinction law derived in this work (eq. [25], *continuous line*) is compared with the Milky Way (*dashed line*) and the LMC (*dot-dashed line*) extinction laws. The extinction law derived by Kinney et al. (1994b) is also shown (*dotted line*). The zero point of the four curves is arbitrary and has been chosen to be the value $Q(5500) = 0.0$.

Extinction vs. Attenuation

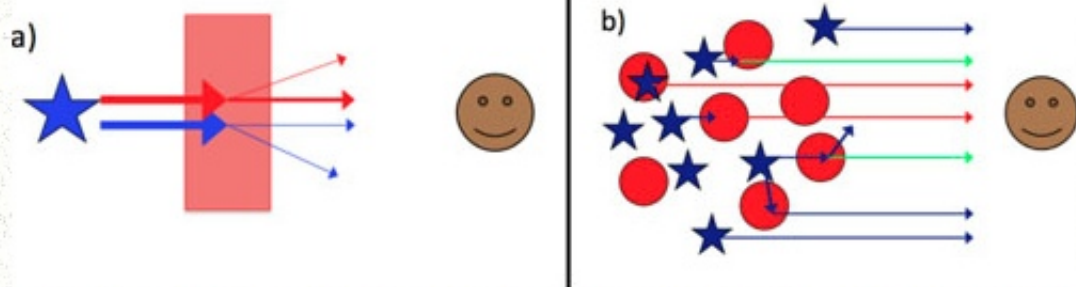
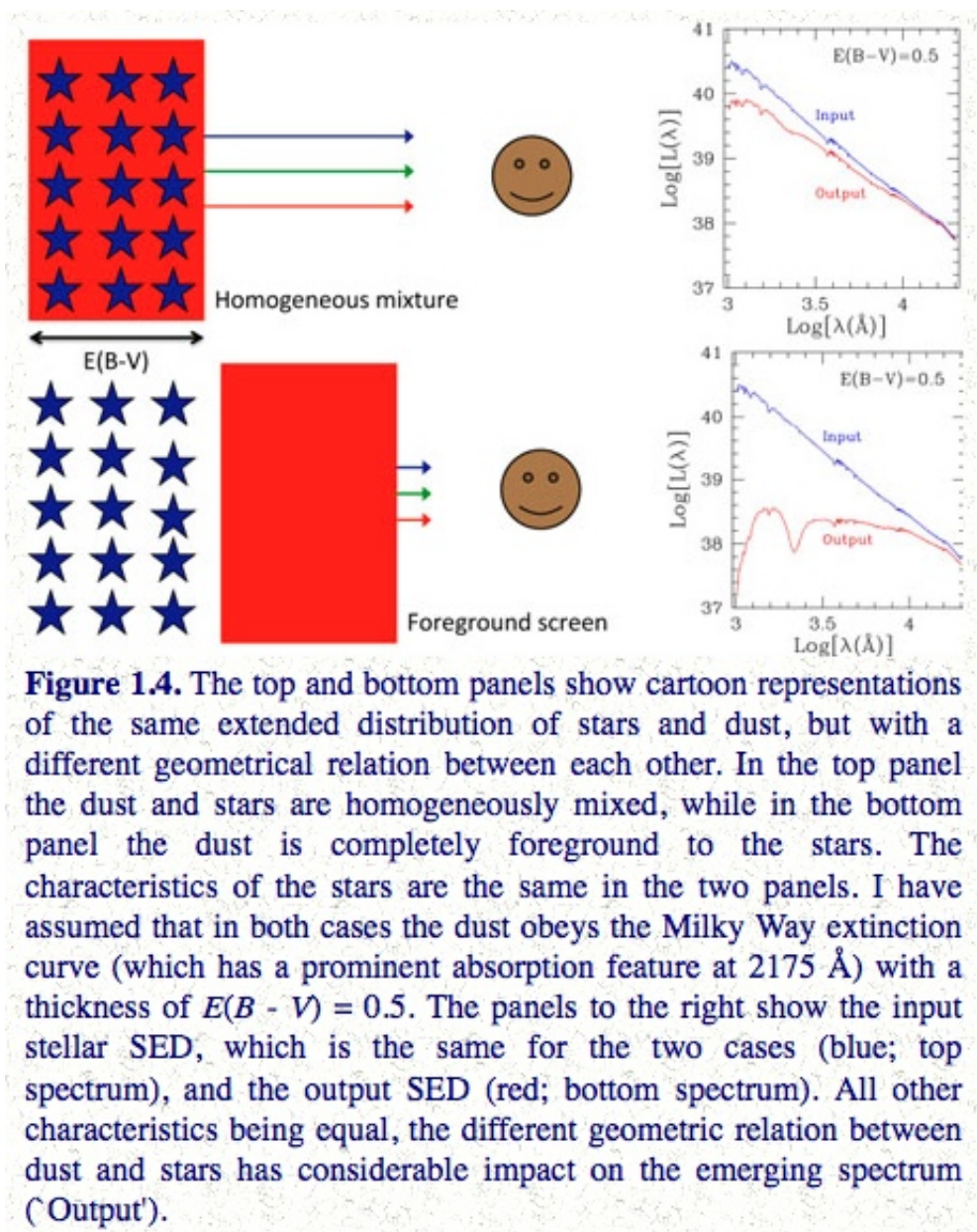


Figure 1.3. The left (a) and right (b) panels are cartoon representations of: a) a point source (star) behind a screen of dust; and b) an extended distribution of stars mixed with clumps of dust. The left panel shows the typical configuration that enables measures of *extinction curves*: a single illuminating source located in the background of the dust. The dust extinguishes the light via direct absorption and via scattering out of the line of sight. The right panel is more representative of the situation encountered whenever a complex distribution of stars and dust is present, as found in external galaxies and large regions. In this case, different stars may encounter different numbers of dust clouds (differences in optical depth), and some stars can be entirely embedded in dust (internal extinction) or be completely foreground to the dust distribution. Scattering of the light by dust both *into* and *out of* the line of sight is present. Because of the more complex geometrical relation between dust and the illuminating sources, the net effect of dust on the stellar population's SED is termed *attenuation*.



http://ned.ipac.caltech.edu/level5/Sept12/Calzetti/Calzetti1_4.html

DUST EXTINCTION OF THE STELLAR CONTINUA IN STARBURST GALAXIES:
THE ULTRAVIOLET AND OPTICAL EXTINCTION LAW

DANIELA CALZETTI AND ANNE L. KINNEY^{1,2}

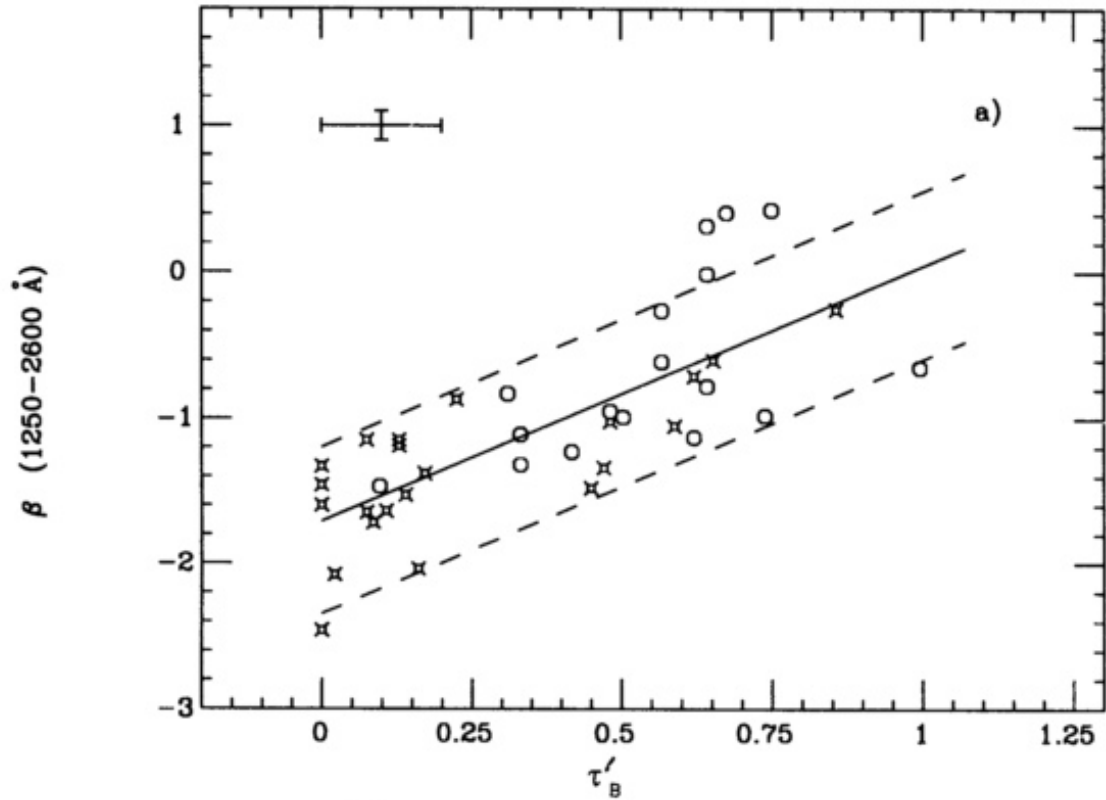
Space Telescope Science Institute, 3700 San Martin Drive, Baltimore MD 21218

AND

THAISA STORCHI-BERGMANN²

Instituto di Fisica, Universidade Federal Rio Grande do Sul, Brazil

Received 1993 August 6; accepted 1994 January 14



$$\tau_B^l = \tau_\beta - \tau_\alpha = \ln \left(\frac{H\alpha/H\beta}{2.88} \right),$$

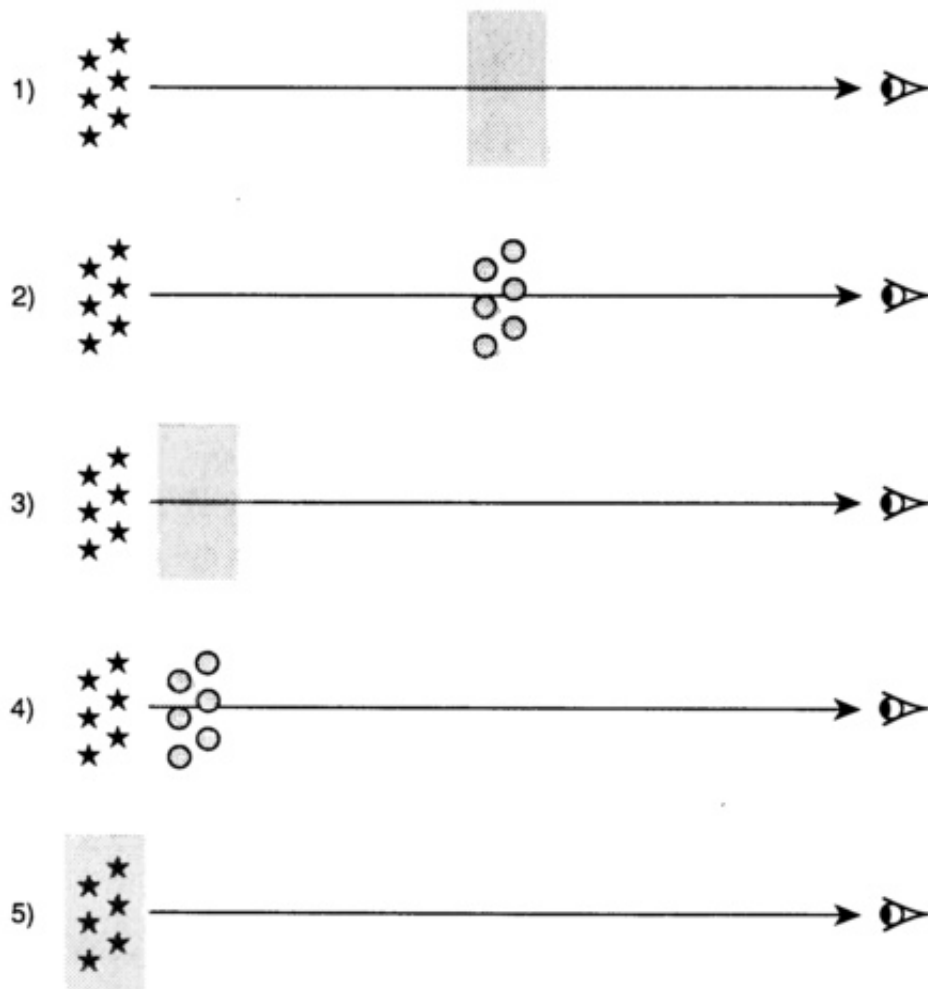


FIG. 8.—A schematic representation of the five configurations of dust/ionized gas discussed in § 4. From top to bottom, they are (1) the uniform dust screen; (2) the clumpy dust screen; (3) the uniform scattering slab; (4) the clumpy scattering slab; (5) the internal dust model.

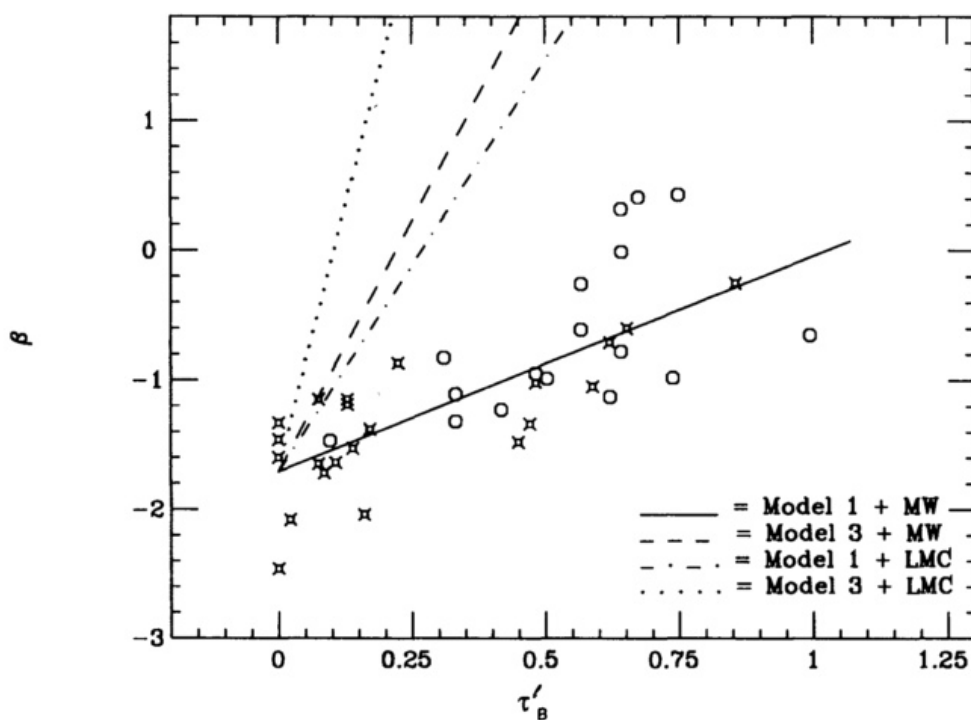


FIG. 12.—The data of β vs. τ_B^l are compared with the curves obtained for the uniform distribution of dust in the absence (model 1) and in the presence (model 3) of scattering of photons into the line of sight. Both the cases of a MW extinction law and an LMC extinction law are considered.

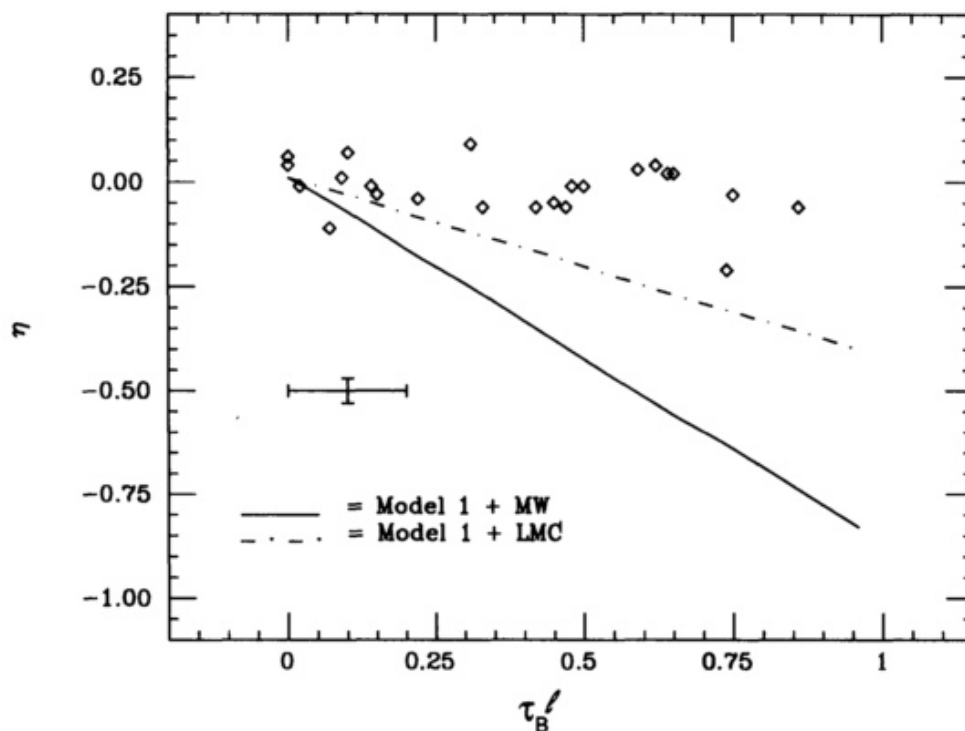


FIG. 13.—The “depth” of the 2175 Å dust bump, η (see eq. [23]), is shown as a function of the Balmer optical depth τ_B^I for our data (*diamonds*), and for the case of a uniform dust screen with MW (*solid line*) and LMC (*dot-dashed line*) extinction law. The formal 1σ error bar on the data is also shown. Our sample contains 24 galaxies for which short and long wavelength *IUE* spectra are available, but NGC 6221 has been excluded from the analysis because of its noisy spectrum.

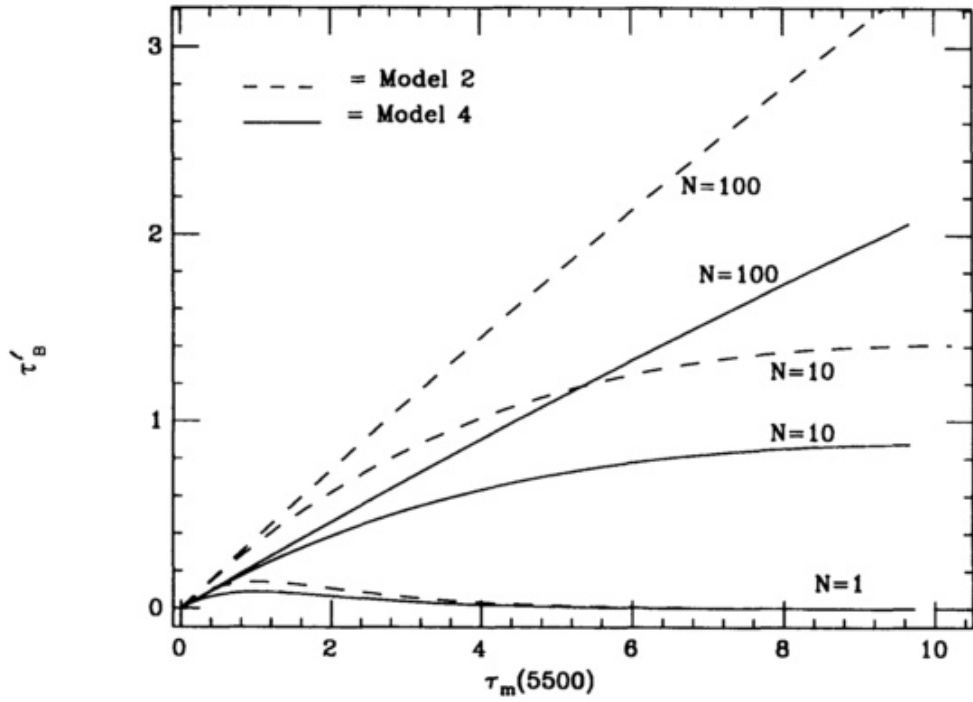


FIG. 14.—The values of the Balmer optical depth τ_B^l are shown as a function of the average optical depth τ_m at 5500 Å for clumpy dust distribution with $\mathcal{N} = 100, 10, 1$, both the absence (model 2) and in the presence (model 4) of scattering of photons into the line of sight. The MW and LMC extinction laws coincide in the optical wavelength range, therefore, the derived τ_B^l are the same for both curves.

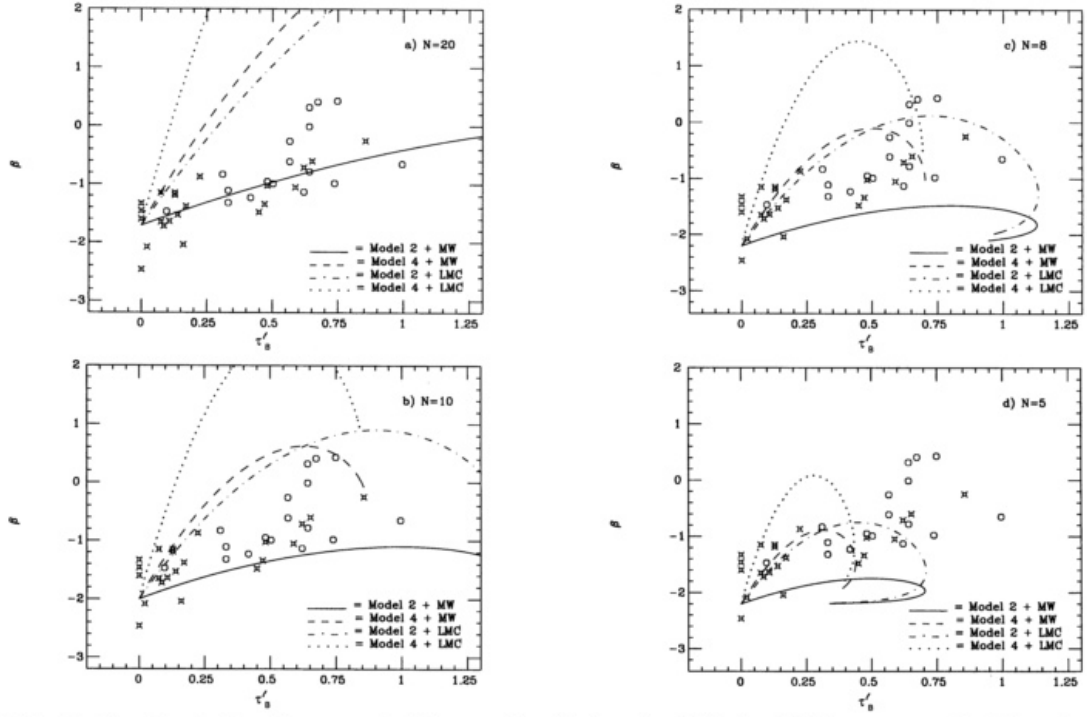


FIG. 15.—The data on β as a function of τ_s^i are compared with the expected trend for clumpy dust distributions with different average number of clumps along the line of sight: (a) $\mathcal{N} = 20$, (b) $\mathcal{N} = 10$, (c) $\mathcal{N} = 8$, (d) $\mathcal{N} = 5$. Both the presence (model 4) and the absence (model 2) of scattering of photons into the line of sight are considered. The MW and LMC extinction curves are used.

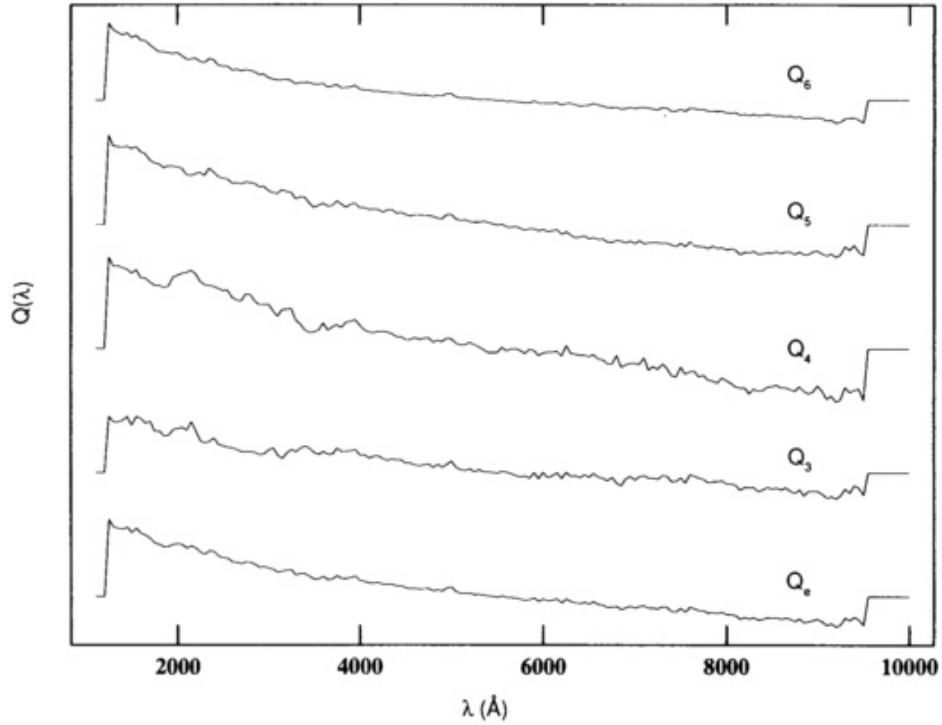


FIG. 19.—The effective extinction law $Q_e(\lambda)$ is compared with the extinction law derived from each single template $Q_n(\lambda)$, with $n = 3, 4, 5, 6$.

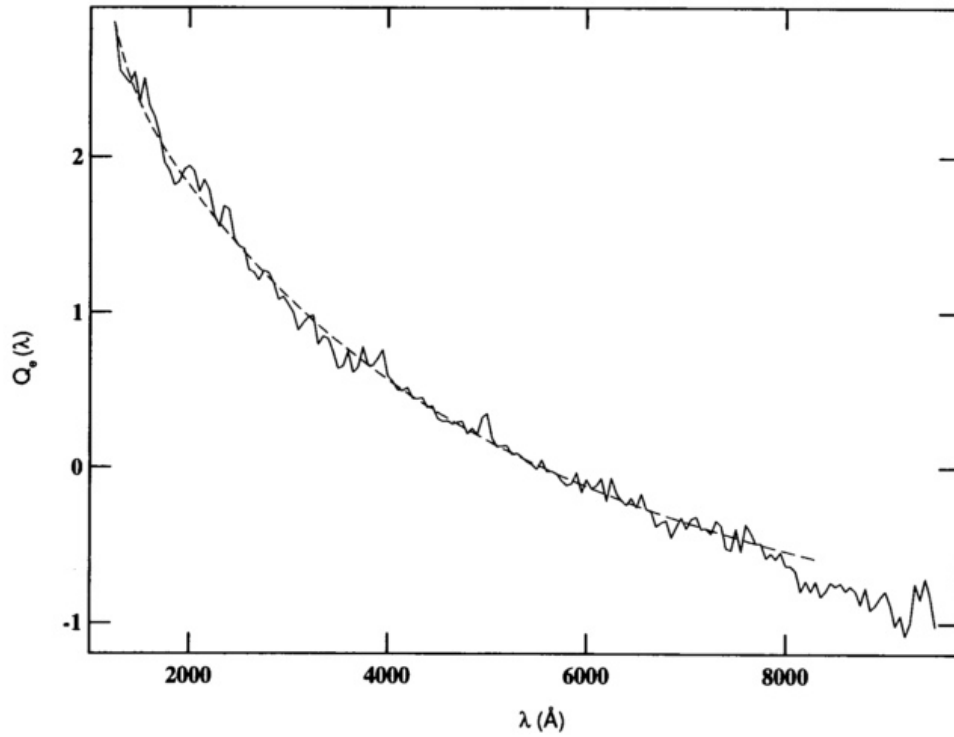


FIG. 20.—The effective extinction law $Q_e(\lambda)$ is shown together with its best fit overplotted in the wavelength range 1250–8000 Å.

Witt & Gordon 2000:

MULTIPLE SCATTERING IN CLUMPY MEDIA. II. GALACTIC ENVIRONMENTS

ADOLF N. WITT

Ritter Astrophysical Research Center, University of Toledo, Toledo, OH 43606; awitt@dusty.astro.utoledo.edu

AND

KARL D. GORDON¹

Department of Physics and Astronomy, Louisiana State University, Baton Rouge, LA 70803; gordon@dirty.phys.lsu.edu

Received 1999 March 12; accepted 1999 July 22

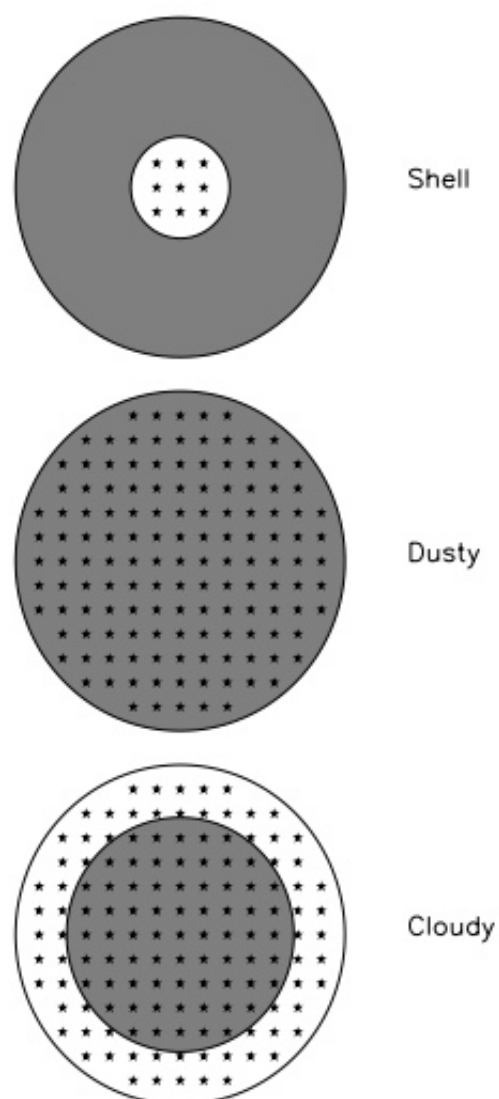


FIG. 1.—Pictorial representation of the three geometries used in this paper (SHELL, DUSTY, and CLOUDY). The star symbols trace the stellar distribution and the grey solid regions give the dust distribution.

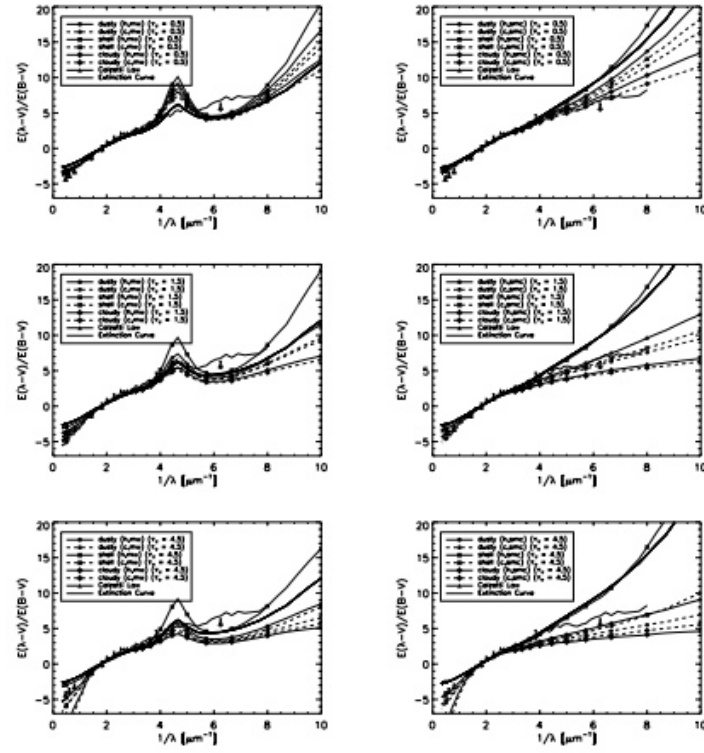
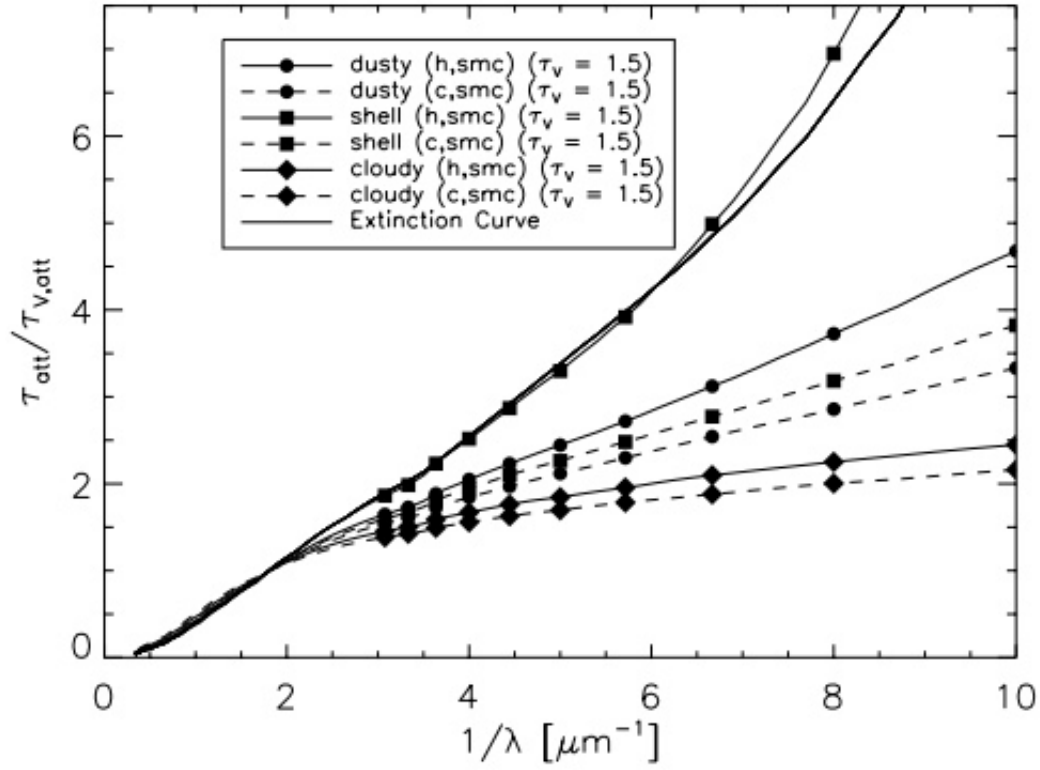


FIG. 9.— $E(\lambda - V)/E(B - V)$ curves for MW and SMC are plotted along with the Calzetti (1997) data derived from starburst galaxies



DUST ABSORPTION AND THE ULTRAVIOLET LUMINOSITY DENSITY AT $z \approx 3$ AS CALIBRATED BY LOCAL STARBURST GALAXIES¹

GERHARDT R. MEURER AND TIMOTHY M. HECKMAN

Department of Physics and Astronomy, Johns Hopkins University, Baltimore, MD 21218-2686; meurer@pha.jhu.edu, heckman@pha.jhu.edu

AND

DANIELA CALZETTI

Space Telescope Science Institute, 3700 San Martin Drive, Baltimore, MD 21218; calzetti@stsci.edu

Received 1998 August 17; accepted 1999 March 22

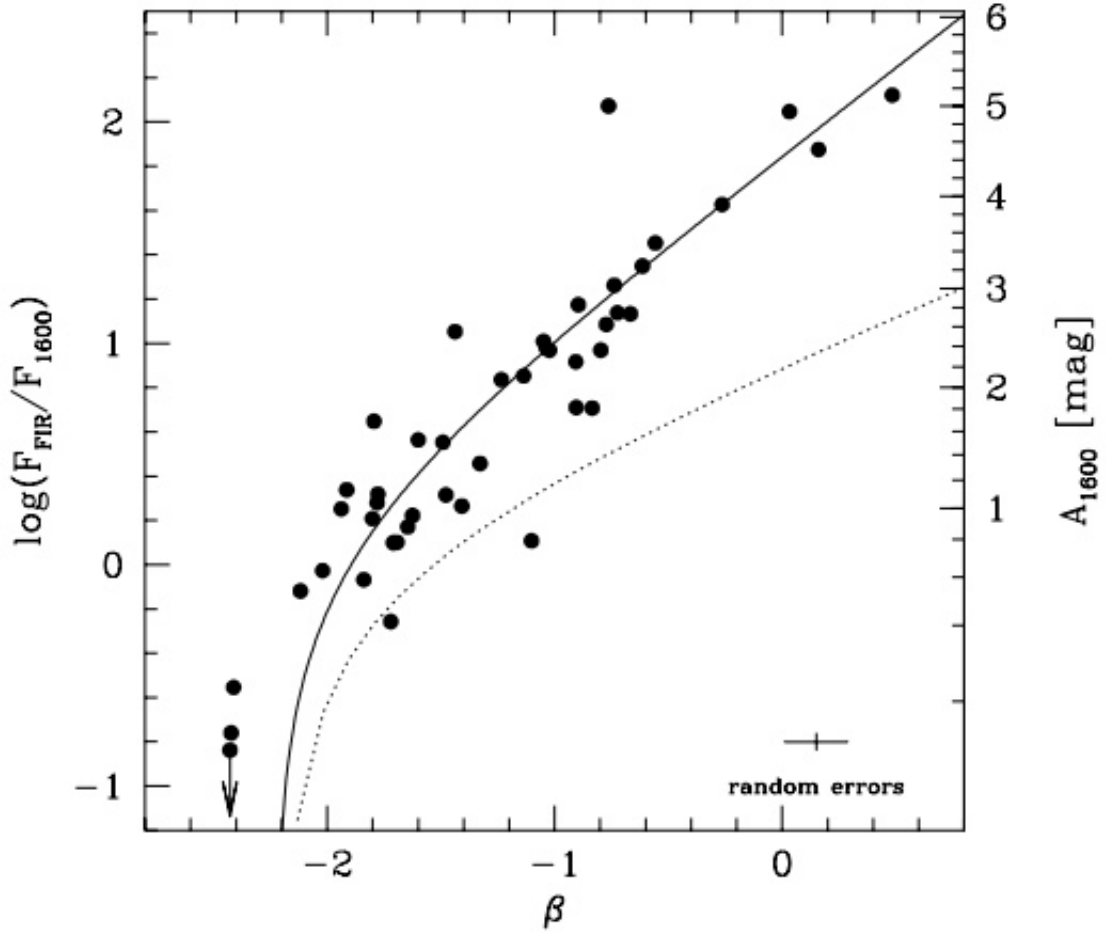


FIG. 1.—Ratio of FIR to UV flux at 1600 Å compared to UV spectral slope β for UV-selected starburst galaxies. The right axis converts the flux ratio to 1600 Å absorption A_{1600} using eq. (11). The solid line shows our adopted linear fit to the A_{1600} - β relationship. The dotted line shows the proposed dust-absorption/population model of Pettini et al. (1998).

$$\text{IRX}_{1600} \equiv \frac{F_{\text{FIR}}}{F_{1600}} = \frac{F_{\text{Ly}\alpha} + \int_{912 \text{ \AA}}^{\infty} f_{\lambda',0} (1 - 10^{-0.4 A_{\lambda'}}) d\lambda'}{F_{1600,0} 10^{-0.4 A_{1600}}} \left(\frac{F_{\text{FIR}}}{F_{\text{bol}}}_{\text{Dust}} \right), \quad (3)$$

where $f_{\lambda,0}$ is the unattenuated flux density of the emitted spectrum, A_{λ} is the net absorption in magnitudes by dust as a function of wavelength, and $F_{\text{Ly}\alpha}$ is the Ly α flux. In our models $F_{\text{Ly}\alpha}$ is derived from the spectrum shortward of 912 Å using the standard assumption that each ionizing photon results in one recombination and consequent decay down to case B population levels. Customarily one adopts a form of

For dust heating well approximated by young stellar populations:

Equation (4) can be rewritten as

$$\text{IRX}_{1600} = (10^{0.4 A_{1600}} - 1) B, \quad (5)$$

where B is the ratio of the two bolometric-like corrections:

$$B = \frac{\text{BC}(1600)_*}{\text{BC}(\text{FIR})_{\text{Dust}}}, \quad (6)$$

where

$$\text{BC}(1600)_* = \left(\frac{F_{\text{Ly}\alpha} + \int_{912 \text{ \AA}}^{\infty} f_{\lambda',0} d\lambda'}{F_{1600,0}} \right)_* \quad (7)$$

and

$$\text{BC}(\text{FIR})_{\text{dust}} = \left(\frac{F_{\text{bol}}}{F_{\text{FIR}}}_{\text{Dust}} \right). \quad (8)$$

$$A_{1600} = 4.43 + 1.99\beta.$$

Casey+2014 provides good review of IRX-beta (see section 2 for references)

- International Ultraviolet Explorer used for UV measurement for original IRX-beta relation but small field of view meant that total UV fluxes underestimated -> revised relation e.g. Takeuchi+ 2012
- Different types of galaxies inhabit slightly different regions of the IRX-beta plane
 - Young, metal-poor SMC and LMC -> redder + less dusty than starbursts.
 - 'Normal' galaxies somewhere between SMC and compact blue starbursts.
 - SFHs (Kong+ 2004) or dust geometries (Cortese+ 2006) both suggested as reasons for these differences.

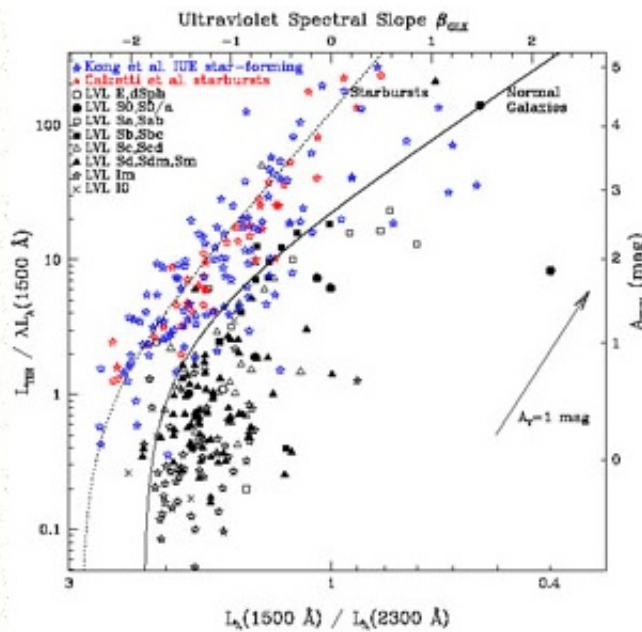


Figure 1.5. The IRX- β plot for local starburst and star-forming galaxies, from [Dale et al. \(2009\)](#). The vertical axis is the IR excess over the UV, where the UV is the *GALEX* FUV (0.15 μ m) band. The horizontal axis is the *GALEX* FUV-NUV colour, expressed as luminosity ratio, with the corresponding values of the UV spectral slope β shown at the top of the plot. The red points are the UV-bright starburst galaxies used by [Meurer et al. \(1999\)](#) to derive the IRX- β relation, shown by the dotted line (Equation 1.22). The blue and black points give the location of normal star-forming galaxies from samples of the local Universe. These galaxies have a much larger spread in the IRX- β plane than the UV-bright starbursts, and typically lower IR excesses at constant UV slope. Their mean trend is shown by the continuous line. An $A_V = 1$ mag attenuation vector is also shown. Reproduced with permission from [Dale et al. \(2009\)](#).

Important points:

- Starburst attenuation curves use the fact that starburst spectra likely to have similar intrinsic slopes to determine law.
- Starburst attenuation curves not suitable for application to non-starburst galaxies because:
 - In the time following the starburst, the ratio of different types of stars contributing to the observed SED will change. Ratios of extinguished and un-extinguished stars to observed SED will change with time dependent on dust geometry within the galaxy.

- Extinction curves built from multiple sightlines to individual stars are different to attenuation curves derived from larger regions.